HHS Public Access

Author manuscript

Mol Carcinog. Author manuscript; available in PMC 2024 July 01.

Published in final edited form as:

Mol Carcinog. 2023 July ; 62(7): 1025–1037. doi:10.1002/mc.23543.

Translational relevance of SOS1 targeting for *KRAS*-mutant colorectal cancer

Diego Alem[1], **Xinrui Yang**[1], **Francisca Beato**[1], **Bhaswati Sarcar**[1], **Alexandra F. Tassielli**[1], **Ruifan Dai**[1], **Tara L. Hogenson**[2], **Margaret A. Park**[1], **Kun Jiang**[3], **Jianfeng Cai**[4], **Yu Yuan**[5], **Martin E. Fernandez-Zapico**[2], **Aik Choon Tan**[6], **Jason B. Fleming**[1], **Hao Xie**[1,†]

[1]Department of Gastrointestinal Oncology, H Lee Moffitt Cancer Center and Research Institute, 12902 USF Magnolia Drive, Tampa, FL 33612

[2]Schulze Center for Novel Therapeutics, Department of Oncology, Mayo Clinic, 200 First Street SW, Rochester, MN 55905

[3]Department of Pathology, H Lee Moffitt Cancer Center and Research Institute, 12902 USF Magnolia Drive, Tampa, FL 33612

[4]Department of Chemistry, University of South Florida, 12111 USF Sweetgum Ln, Tampa, FL 33620

[5]Department of Chemistry, University of Central Florida, 4111 Libra Drive, Orlando, FL 32816

[6]Department of Biostatistics and Bioinformatics, H Lee Moffitt Cancer Center and Research Institute, 12902 USF Magnolia Drive, Tampa, FL 33612

Abstract

Background—It has been challenging to target mutant KRAS (mKRAS) in colorectal cancer (CRC) and other malignancies. Recent efforts have focused on developing inhibitors blocking molecules essential for KRAS activity. In this regard, SOS1 inhibition has arisen as an attractive approach for mKRAS CRC given its essential role as a guanine nucleotide exchange factor for this GTPase. Here, we demonstrated the translational value of SOS1 blockade in mKRAS CRC.

Method—We used CRC patient-derived organoids (PDOs) as preclinical models to evaluate their sensitivity to SOS1 inhibitor BI3406. A combination of *in silico* analyses and wet lab techniques was utilized to define potential predictive markers for SOS1 sensitivity and potential mechanism of resistance in CRC.

[†]Corresponding author Hao Xie, MD, PhD, Department of Gastrointestinal Oncology, H Lee Moffitt Cancer Center and Research Institute, 12902 USF Magnolia Drive, Tampa, FL 33612.
Current address: Division of Medical Oncology, Mayo Clinic, 200 First Street SW, Rochester, MN 55905. xie.hao@mayo.edu; Phone: 507-284-8759

Author contributions

Hao Xie, Aik Choon Tan, and Jason B. Fleming designed this study. Diego Alem, Xinrui Yang, Francisca Beato, Bhaswati Sarcar, Alexandra F. Tassielli, Ruifan Dai, and Tara L. Hogenson performed the experiments. Kun Jiang, Francisca Beato, Ruifan Dai assisted in sample collection and pathology review. Hao Xie and Margaret A. Park analyzed the data. Hao Xie wrote the manuscript. Jianfeng Cai, Yu Yuan, Martin E. Fernandez-Zapico, Aik Choon Tan, Jason B. Fleming, and Hao Xie helped revision of the manuscript, funding acquisition, and project administration. All authors have read and approved the final manuscript.

Conflict of interest

None

Result—RNA-seq analysis of CRC PDOs revealed two groups of CRC PDOs with differential sensitivities to SOS1 inhibitor BI3406. The resistant group was enriched in gene sets involving cholesterol homeostasis, epithelial mesenchymal transition, and TNFα/NFκB signaling. Expression analysis identified a significant correlation between SOS1 and SOS2 mRNA levels (Spearman's ρ 0.56, $p<0.001$). SOS1/2 protein expression was universally present with heterogeneous patterns in CRC cells but only minimal to none in surrounding non-malignant cells. Only SOS1 protein expression was associated with worse survival in patients with *RAS/RAF* mutant CRC ($p=0.04$). We also found that SOS1/SOS2 protein expression ratio > 1 by IHC ($p=0.03$) instead of *KRAS* mutation ($p=1$) was a better predictive marker to BI3406 sensitivity of CRC PDOs, concordant with the significant positive correlation between SOS1/SOS2 protein expression ratio and SOS1 dependency. Finally, we showed that GTP-bound RAS level underwent rebound even in BI3406-sensitive PDOs with no change of KRAS downstream effector genes, thus suggesting upregulation of guanine nucleotide exchange factor as potential cellular adaptation mechanisms to SOS1 inhibition.

Conclusion—Taken together, our results show that high SOS1/SOS2 protein expression ratio predicts sensitivity to SOS1 inhibition and support further clinical development of SOS1-targeting agents in CRC.

Keywords

SOS1; SOS2; KRAS; colorectal cancer; therapeutics

Introduction

Approximately half of metastatic colorectal cancers (CRC) carry driver mutations in the *RAS* family of genes. These genetic alterations are associated with poor responses to standard chemotherapy and serve as negative predictive marker to anti-EGFR blockade.[1] As a result, patients with mRAS CRC have worse outcome and urgently need novel targeted therapy options. For these reasons, there have been significant efforts and advances recently in the development of novel therapeutics either directly inhibiting mKRAS or targeting functionally important downstream effector pathways, namely MAPK and PI3K.[2] However, similar to other targeted agents in clinical practice, set aside issues with primary resistance, development of acquired resistance is inevitable in majority of the cases and toxicities of combination therapies may become prohibitory to tolerate.[3] Thus, these suggest the need for the development of novel strategies to overcome these issues.

SOS1 is a guanine nucleotide exchange factor promoting the production of active GTP-bound RAS.[4] Targeting SOS1 may have advantages over other indirect approaches to *RAS* signaling suppression given its direct protein-protein interaction with RAS.[3] Using CRC patient-derived organoids (PDOs),[5-7] we evaluated the anti-tumoral effects of BI3406, a SOS1 inhibitor, whose clinical counterpart is currently undergoing a Phase I trial alone or in combination with trametinib in advanced solid tumors.[8] The availability of these agents provides the opportunity to specifically target signaling components proximal to mRAS, which allows new combination therapies. In vitro studies showed that SOS1 inhibitor as a single agent is active in cell lines, especially lung cancer cells with *EGFR* and *KRAS G12/13* mutations instead of *KRAS Q61* and *BRAF* type I/II mutations.[9-11] But these

findings lack further validation in patient-relevant models. In contrast to lung cancer, *RAS* signaling in CRC is very different given its intrinsic upregulation of RTK ligands. Hence, to define the translational value of SOS1 inhibition, in this study, we defined new predictive markers for the sensitivity and resistance of SOS1 inhibitor in CRC. We demonstrated the potential values of early adoption of PDOs in the discovery of biomarkers and cellular effects associated with SOS1 inhibitors in mRAS CRC.

Materials and Methods

Patients

Patients were enrolled under prospective protocols approved by Moffitt Cancer Center (MCC) Institutional Review Board including MCC20584 “Generation and *Ex vivo* Testing of Immune-Based Cell Therapy from Gastrointestinal Malignancies” and MCC19990 “Biological determinants of colorectal cancer outcomes in Latinos of diverse ancestral origins”. These protocols allowed the collection of surgically resected tumor specimens including CRC at MCC. Tumor specimens were from either primary or metastatic CRC including but not limited to liver and peritoneal metastases as part of routine clinical care. The use of reagents derived from these tumor specimens was approved under protocol MCC20880 “Preclinical Testing of SOS1 Inhibition and Degradation in *RAS*-Mutant Colorectal Cancer”. Tumor specimens collected were de-identified and assigned a lab number. The type and site of tumor specimen, patient’s demographic and clinical information, treatment history, previous tumor genetic information, and organoid initiation date were collected when available. Patient-derived xenografts (MCC IACUC protocol: 8797R) were used to generate and biobank tumor specimens. The tumor samples were subsequently used to generate additional CRC patient-derived xenografts (PDXs) and PDOs.

Patient-derived organoid (PDO) culture

Briefly, the tumor specimen was minced into approximately 1 mm^3 small fragments using sterile scalpels in fresh wash media. Tissue fragments were placed in warmed digestion media and incubated for 30-45 minutes on a shaker with agitation at 37°C and 600 rpm to allow tissue to dissociate into single cells. Larger tissue fragments were allowed to settle under normal gravity. The supernatant was transferred out followed by an addition of 3 mL wash media with 10% FBS. Cells were filtered through a 100 μM mesh filter and a 40 μM filter to remove mouse fibroblasts. Cell pellets suspended in 300 μL of ice-cold growth factor reduced Matrigel (Corning, 354230), then plated into 50 μL domes in a 24-well pre-warmed culture plate, which was allowed to solidify for 15 minutes at 37°C. When the Matrigel domes solidified, 500 μL of pre-warmed complete growth media was added and incubated in 5% CO_2 atmosphere at 37°C. The growth of the organoids was monitored with fresh growth media change every 2 days. Organoid propagation was performed in a sequence of gentle mechanical digestion followed by enzymatic digestion. The cell pellet was resuspended in wash media with 0.1% BSA, followed by embedment into Matrigel domes. Wash media: advanced DMEM/F12 (Gibco, 12634010), 100X glutamine (Gibco, 25030149), 1M Hepes (Gibco, 15630080), primocin (Invivogen, ANTPM1). Digestion media: wash media/10% FBS, collagenase and dispase (Sigma, 10269638001). Growth media: wash media without FBS, 1X wnt3a/R-spondin/Noggin condition medium (L-

WRN), 100 ng/mL recombinant mouse Noggin (abcam, ab281818), 1X B27 supplement (Gibco, 12587-010), 50 ng/mL hEGF (R&D Systems, 236EG200), 100 ng/mL human FGF (R&D Systems, 233-FB), 10 mM nicotinamide (Sigma Aldrich, N3376), 1.25 mM N-acetylcysteine (Sigma Aldrich, A9165), 100 μg/mL primocin (Invivogen, ANTPM1), 500 nM A83-01 (Selleckchem, S7692), 10.5 μM Y-267632 (Selleckchem, S1049), 10 nM human gastrin I (R&D Systems, 3006/1), and 1 μM PGE2 (R&D Systems, 2296/10).

Establishment of CRC PDXs

NOD/SCID and nude mice (female, aged 6 week) were purchased from Jackson Laboratories. Fresh tumor samples were cut into fragments of about 2–3 mm,[16] briefly soaked in Matrigel, and then implanted in the subcutaneous space of the mice.[17,18] Tumors were measured weekly. Tumor volumes were calculated using the formula length × width^2 × 0.52. The tumors were harvested when they reached 0.75-1.5 cm in diameter and labeled F1 to F4 to indicate different generational passages in animals. To estimate and compared CRC PDX tumor growth, area under the tumor growth curve up to time t (aAUC) was calculated using R script with access provided by cgc@sbgenomics.com.[19]

Patient-derived organoid (PDO) culture

CRC organoids were generated and expanded using a protocol like previously published protocols for CRC with modifications (refer to Supplemental Methods for details).[7,20,21]

Organoid drug sensitivity assay

Organoids were harvested with organoid cell recovery solution (Corning, 354253) and pipetted gently to dissolve Matrigel. After incubation for 15 minutes, the cells were collected and washed with 0.1% BSA/wash media, followed by resuspension in a mixture of 90% complete growth media and 10% Matrigel. Cells were seeded in triplicates into a 96-well plate previously prepared with solidified 30 μL of 50% Matrigel and 50% complete growth media in each well. Once the organoids were visible after 3-7 days, drugs were added and cultured for 72 hours. Chemiluminescence was read at 360/460 nm on an Envision multi-well plate reader (PerkinElmer) after addition of CellTiter-Glo 3D (Promega, G9681). After normalization to 0.2% DMSO-treated cells, dose-response curves were generated with IC_{50} values calculated using GraphPad Prism 8.4.3.

Immunohistochemistry of tumor tissue for SOS1 and SOS2

SOS1 and SOS2 IHC procedures are described in detail in Supplemental Methods. Slides were reviewed by a gastrointestinal pathologist (K. J.) who adopted a semiquantitative scoring system of IHC results as previously described.[22] Briefly, percentage of positively stained cells was assigned a score as 0 = 0%, 1 = <30%, 2 = 30-60%, 3 = >60%. Intensity of IHC stain was assigned a score as 0 = no reaction, 1 = weak, 2 = mild, 3 = strong. Multiplication of the two scores provided the final score.

Ras GTPase level in PDOs

Ras GTPase Chemi ELISA Kit (Active Motif, 52097) was used to measure Ras GTPase level in organoids. The assay was performed according to the manufacture's manual. Briefly,

organoids were treated with 1 μM BI3406 and harvested at different time points (0, 6, 24 and 48 hours) for the preparation of whole-cell extract. GST-Raf-RBD diluted in complete lysis binding buffer was added to each well. The plate was incubated for 1 hour at 4°C. Test extract diluted in complete lysis/binding buffer along with positive control extract (EGF treated HeLa) and complete lysis/binding buffer were added to the corresponding wells. Diluted Ras antibody, specific for human HRAS and KRAS, was added to the wells. The plate was incubated for 1 hour at room temperature. Diluted HRP antibody was added to all wells. The plate was then incubated for 1 hour at room temperature, followed by addition of chemiluminescent working solution. The chemiluminescence was read by a luminometer.

RNA-sequencing and data analysis

RNA extracted from cells was quantitated with the Qubit Fluorometer (ThermoFisher Scientific, Waltham, MA) and screened for quality on the Agilent TapeStation 4200 (Agilent Technologies, Santa Clara, CA). The samples were then processed for RNA-sequencing using the NuGEN Universal RNA-Seq Library Preparation Kit with NuQuant (Tecan Genomics, Redwood City, CA). Briefly, 100 ng of RNA was used to generate cDNA and a strand-specific library following the manufacturer's protocol. Quality control steps were performed, including TapeStation size assessment and quantification using the Kapa Library Quantification Kit (Roche, Wilmington, MA). The final libraries were normalized, denatured, and sequenced on the Illumina NextSeq 2000 sequencer with the P3-200 cycle reagent kit to generate approximately 50M million 100-base read pairs per sample (Illumina, Inc., San Diego, CA).

Read adapters were detected using BBMerge (v37.88)[23] and subsequently removed with cutadapt (v1.8.1)[24]. Processed raw reads were then aligned to human genome HG38 using STAR (v2.5.3a).[25] Gene expression was evaluated as read count at gene level with RSEM (v1.3.0)[26] and Ensembl Gencode gene model v32. Gene expression data were then normalized and differential expression between experimental groups were evaluated using DEseq2.[27] Pathway enrichment were analyzed with gene set enrichment analysis (GSEA)[28] using MSigDB Hallmark gene sets.

Database used for analyses

We analyzed relevant publicly available CRC datasets in this study to determine the association of SOS1 with clinical and functional outcomes. These datasets include GENIE cohort v11.0, https://genie.cbioportal.org/.[29,30] DFCI CRC cohort, https://www.cbioportal.org/study/summary?id=coadread_dfci_2016.[31] TCGA PanCancer Atlas CRC cohort, https://www.cbioportal.org/study/summary?id=coadread_tcga_pan_can_atlas_2018.[32] CPTAC-2 Prospective, https://www.cbioportal.org/study/summary?id=coad_cptac_2019.[33] DepMap, https://depmap.org/portal/.[34]

Statistical analysis

Statistical analysis for this study was descriptive in nature without sample size or power calculation. Categorical data were summarized as frequency counts and percentages and compared with χ^2 or Fisher's exact test. Continuous data were summarized as means,

standard deviations, standard errors, medians, and ranges and compared with independent t test or Mann-Whitney U test. For variables with more than two categories, they were compared with one-way ANOVA or Kruskal-Wallis test. Correlation between variables were assessed with Spearman's rho. All statistical tests were 2-sided with $p < 0.05$ considered statistically significant. For the GSEA and gene co-occurrence results, a q-value <0.05 yields a false discovery rate (FDR) of 5% will be called significant. Overall survival (OS) was calculated from the date of tumor resection to the date of death. Surviving patients were censored at the date of last follow-up. Time-to-event data were summarized using Kaplan-Meier method and compared with log-rank tests. Statistical analyses were performed using either GraphPad Prism 8.4.3 or R version 4.2.0.

Results

Differential gene expression and sensitivity to SOS1 inhibition in CRC PDOs

To evaluate the translational role of SOS1 inhibition in mRAS CRC, we used PDOs derived from surgically resected tumor samples of patients with distinct age, race, gender, tumor location, tumor stage, and microsatellite/mismatch repair protein status (Supplemental Table 1). We performed RNA-sequencing (RNA-seq) followed by differential gene expression analysis of these CRC PDOs at baseline and found that they can be classified into group 1 (MCC19990-006, MCC19990-010, and MCC19990-013) and group 2 (MCC19990-002, MCC19990-007, and MCC20584-010) (Figure 1A). Interestingly, we found that group 1 PDOs were more sensitive to SOS1 inhibition; in contrast, group 2 PDOs were more resistant to SOS1 inhibition (Figure 1B). With all the CRC PDOs considered, they had differential responses to SOS1 inhibitor BI3406 as shown in Figure 1C. Analysis of the GTP-bound RAS level had a rebound at 48 hours despite various levels of initial suppression upon treatment with BI3406 in both SOS1-inhibitor resistant (MCC19990-002, MCC19990-007) and sensitive (MCC19990-010) CRC PDOs (Figure 1D). This observation was supported by that fact that expressions of the 9 *KRAS* effector genes in the 3 BI3406-sensitive CRC PDOs after treatment with BI3406 for 24 hours did not show significant difference (Figure 1E) despite suppression of some enriched gene sets such as E2F and MYC Targets (Figure 1F). Finally, given the functional role of *RAS* pathway activation by epidermal growth factor (EGF) in CRC and recently report on the effect of culture media composition on the predictive ability to treatment response by PDOs of gastrointestinal cancers,[35] we looked at the effect of human EGF, routinely present in the culture media, on SOS1 inhibitor sensitivity in a sensitive and resistant CRC PDO (Figure 1G). We found no significant effect of human EGF on SOS1 inhibitor sensitivity. The range of IC_{50} values to BI3406 was between 0.53 μM and 45.9 μM among 9 CRC PDOs with wild type and various *KRAS* mutations (Figure 1B). As shown in Figure 1H, the IC_{50} values of BI3406 in BI3406-sensitive CRC PDOs are significantly lower than those in BI3406-resistant CRC PDOs (p=0.016). Together, these results showed that the cellular effect of SOS1 inhibition have implications that go beyond the suppression of *KRAS* signaling.

The prognostic value of SOS1 in CRC

In order to define potential biomarkers predicting SOS1 inhibition, we investigated the molecular alterations associated with SOS1 in CRC using *in silico* analysis of large CRC

datasets. In the GENIE cohort (n=5790), the prevalence of SOS1 mutations across different cancer types is generally very low with 2.9% in CRC (Figure 2A). It is not statistically different across different tumor stages (p=0.2), primary versus metastatic sites (p=0.07), or left versus right sided CRC (p=0.3) (Supplemental Figure 1A-C). The prevalence of SOS1 mutations is much lower than that in common clinically relevant genes such as *KRAS*, *BRAF*, and *HER2*. In addition, SOS1 has co-occurrence with these genes (q<0.001) (Supplemental Figure 1D) in addition to its co-occurrence with its paralog SOS2 (q=0.03) (Supplemental Figure 1E). As to the function of SOS1 mutations, distribution of *SOS1* alterations in CRC of the GENIE cohort was visualized and only 1 of 185 (0.5%) *SOS1* alterations was determined by OncoKB and hotspots as a putative driver of CRC (Figure 2B).

As to *SOS1* mRNA expression, there was no statistical difference between *RAS/RAF* wild-type and *RAS/RAF* mutant CRC (p=0.3) and across different tumor stages (p=1) in the TCGA PanCancer Atlas CRC cohort (n=578) (Supplemental Figure 1F-G). However, there was a significant correlation between *SOS1* and *SOS2* mRNA expression levels with Spearman's ρ of 0.56 (p<0.001) (Figure 2C). Similarly, SOS1 protein was not differentially expressed between *RAS/RAF* wild-type and mutant CRC (p=0.3) and across different tumor stages (p=0.4) in the CPTAC-2 CRC cohort (n=89) (Supplemental Figure 1H-I). There was only a trend of correlation between SOS1 and SOS2 protein express levels (Spearman's ρ 0.45, p=0.1) (Supplemental Figure 1J), maybe partially due to small sample size or the lack of correlation between *SOS1* mRNA and SOS1 protein expression levels (Spearman's ρ −0.05, p=0.6) (Figure 2D). We further evaluated SOS1 and SOS2 protein expression by immunohistochemistry (IHC) in surgically resected CRC tissues. SOS1 and SOS2 were universally expressed in cancer cells with only minimal to no SOS1 and SOS2 expression in surrounding non-malignant tissues (Figure 2E-F). SOS1 and SOS2 expressions patterns including nuclear, cytoplasmic, and likely inner membranous expressions were also very different in morphologically distinct CRC specimens (Figure 2G-H). In addition, the expression levels of SOS1 and SOS2 are not always correlated as assessed by IHC.

Further evaluation of SOS1 and SOS2 protein expression by IHC in CRC PDX models showed that their expression levels and SOS1/SOS2 protein expression ratio remained rather stable across PDX generational passages 1 through 3 (Supplemental Figure 2A-C), between primary and metastatic CRC models (Supplemental Figure 2D-F), and between *KRAS* wild-type and mutant CRC PDX models (Supplemental Figure 2G-I). We quantified our CRC PDX tumor growth using adjusted AUC (aAUC) and found that neither SOS1 or SOS2 protein expression levels nor SOS1/SOS2 protein expression ratio group (elevated if ratio >1, not elevated if ratio≤1) were associated with CRC PDX tumor growth (Supplemental Figure 2J-L). Of note, CRC PDX tumor growth was not associated with *KRAS* mutation status (p=0.5) or primary versus metastatic CRC (p=0.8), either.

In contrast, in the CPTAC-2 CRC patient cohort, when SOS1 protein expression level measured by mass spectrometry was dichotomized using Z-score 0 as a cutoff, SOS1 high group (38 cases and 5 events) had significantly worse OS (p=0.048) compared to SOS1 low group (52 cases and 2 events) (Supplemental Figure 3A). Similarly, in patients with *RAS/RAF* mutant CRC, SOS1 high group has significantly worse OS (p=0.04) compared

to SOS1 low group (Supplemental Figure 3B). However, when similar analyses were performed for *SOS1* mRNA expression, higher *SOS1* mRNA expression was not associated with OS in the entire cohort (p=0.2) or patients with *RAS/RAF* mutant CRC (p=0.051) (Supplemental Figure 3C-D). In summary, SOS1 protein is preferentially expressed in CRC cells and is a poor prognostic marker in CRC.

Predictive markers to SOS1 inhibitor sensitivity in CRC PDOs

Given previous report on the association between *KRAS G12/G13* mutations and BI3406 sensitivity, we treated our CRC PDO models with BI3406 as shown previously (Figure 1B) and found that CRC PDOs, either *KRAS* mutant or *KRAS* wild type had responses to BI3406 equally (p=1) (Figure 3A). In addition, interrogation of the DepMap database for the dependency of CRC cell lines to common genes in *KRAS* pathway showed that cells that are more dependent on *SOS1* do not have *KRAS* driver mutations (Figure 3B). There was no correlation (Spearman's ρ 0.18, p=0.2) between *SOS1* and *KRAS* dependency scores in CRC cell lines (Figure 3C). Further analysis of gene expressions of CRC cell lines with differential sensitivities (3 sensitive and 5 resistant) to BI3406 as defined by Hoffmann et al.[10] identified gene features that were able to distinguish sensitive CRC cell lines from resistant ones (Supplemental Figure 4A). GSEA identified 9 gene sets that are significantly enriched in BI3406-sensitive cell lines at nominal p<0.01 including E2F and MYC Targets (Supplemental Figure 4B). Similar observations were found in CRC cell lines with differential *SOS1* dependencies (8 dependent and 40 independent) as defined by CRISPR knockout experiments (Supplemental Figure 4C) along with 17 gene sets significantly enriched in *SOS1*-dependent CRC cell lines at nominal p<0.01 including Interferon Alpha and Gamma Responses (Supplemental Figure 4D). With further GSEA of CRC cell lines based on their *KRAS* dependency, we found that only a proportion of the enriched gene sets are shared among BI3406-sensitive, *SOS1* dependent, and *KRAS* dependent CRC cells (Supplemental Figure 4E). In summary, *KRAS* mutations may not be a good predictive marker to either SOS1 inhibitor sensitivity or *SOS1* dependency (genetic knockout) in mRAS CRC.

We then evaluated the potential of SOS1 and SOS2 protein expressions as predictive markers. We found that higher SOS1/SOS2 protein expression ratio in CRC cell lines measured by mass spectrometry was significantly associated *SOS1* dependency (Spearman's ρ −0.886, p=0.007) (Figure 3D) instead of SOS1 protein expression, *SOS1* or *SOS2* mRNA expression or their ratio (Supplemental Figure 5A-C). Higher SOS1/SOS2 protein expression ratio by IHC in our CRC PDOs predicted sensitivity to BI3406 (p=0.04) (Figure 3E). Practically, all cases in SOS1/SOS2 expression ratio elevated group defined as SOS1/SOS2 H-score ratio >1 were sensitive to SOS1 inhibition by BI3406 (p=0.03) (Figure 3F). Neither SOS1 nor SOS2 protein expression alone was associated with BI3406 sensitivity (Supplemental Figure 5D-E).

In addition, GSEA of our RNA-sequencing results of CRC PDOs identified 7 gene sets significantly enriched at nominal p<0.01 in BI3406 resistant CRC PDOs (Figure 4A) with the top three including Cholesterol Homeostasis, Epithelial Mesenchymal Transition, and TNFα-NFκB (Figure 4B), which could also be investigated and validated in the

future as potential predictive markers for sensitivity to SOS1 inhibition. Together, these results showed that SOS1/SOS2 protein expression ratio could predict sensitivity to SOS1 inhibition and pathways other than KRAS may be involved in primary resistance to SOS1 inhibitor in mRAS CRC.

Discussion

In this study, we defined the translational value of SOS1 targeting in *KRAS*-mutation CRC. *SOS1* activating mutations have been reported in Noonan's syndrome and other RASopathies.[36-38] However, driver mutations were reported to be rare like what we found in CRC.[39] Therefore, *SOS1* mutations are unlikely to be responsible for the pathogenesis of a subset of CRC or used as prognostic or predictive markers. The findings on the positive correlation between SOS1 and SOS2 mRNA and protein expressions supported previous hypotheses on similar GEF function for RTK-dependent RAS activation by SOS2. SOS2 may be more related to PI3K signaling instead of MAPK signaling. The latter is more regulated by SOS1.[11,40] However, no SOS2 inhibitor is available to date despite that SOS2 inhibition may be more effective in suppression of *RTK/RAS* signaling.[11,40] In an effort to tease out the relationship between SOS1 and SOS2 protein expressions, we immunochemically stained them in specimens from patients with CRC. Universal expression in tumor tissue along with minimal expression in surround normal tissue supported that SOS1 has the potential to be a selective target in CRC sparing the on and off target toxicities in normal tissue. However, we also noticed that the patterns and levels of SOS1 and SOS2 expressions in CRC with different morphologies are highly heterogeneous which warranted further investigations on their functional significance in future studies with larger sample size. SOS1 and SOS2 protein expressions by IHC were stable without significant changes across CRC PDX passages, histopathologic, and genetic variables, which supported their potential as robust biomarkers. Higher SOS1 protein expression as a poor prognostic marker for survival in a small cohort of patients with CRC, although requiring further validation in a larger cohort, yet provided the rationale to target SOS1 for inhibition or degradation.

The development of companion predictive biomarker has played critical role in the clinical success of targeted therapy and optimal patient selection in key clinical trials. More recent examples in CRC include the use of predictive biomarkers to guide the use of anti-HER2 therapy and KRAS G12C inhibitors. In our effort to discover predictive biomarkers to the sensitivity of SOS1 inhibitor, we surprisingly did not find *KRAS G12/13* mutations as a predictive marker to either SOS1 inhibition or dependency in CRC. This observation could be a result of several contributing factors: 1) previous studies[10] involved simultaneous studies of different tumor types where each one has different tumor biology. For example, EGFR-mutation is essential for RAS activation in lung cancer where SOS1 inhibition is synergistic with EGFR-TKIs. This is clearly not the case in CRC; 2) different tumor models were used where cell line models without patient-relevance were less likely to inform predictive biomarker discovery; 3) the presence of other co-mutations as reported previously,[10,41] and 4) off-target activities of SOS1 inhibitor used, which was supported by the fact that different gene sets were enriched among BI3406-sensitive, *SOS1*-dependent, and *KRAS*-dependent CRC cell lines. Gratifyingly, we found that SOS1/SOS2 protein expression ratio by IHC in CRC tissues was correlated with BI3406 sensitivity of CRC

PDOs derived from the same tissue specimen. This finding was independently confirmed by DepMap data showing SOS1/SOS2 protein expression ratio by mass spectrometry was highly correlated with *SOS1* dependency in CRC cell lines. This observation was in concordant with the role of SOS2 as a compensation mechanism to the suppression of SOS1 function. In cases where SOS2 protein was less expressed or knocked down, the cancer cells became more sensitive to SOS1 inhibition.[10] The comparison of mRNA expressions in SOS1 inhibition sensitive and resistant CRC PDOs revealed distinct genes and gene sets which could serve as additional predictive markers for BI3406 sensitivity or primary resistance mechanisms which could provide insights in combination therapy development. The top three gene sets enriched in BI3406-resistant CRC PDOs including cholesterol homeostasis,[42] epithelial mesenchymal transition[43] and TNFα/NFκB,[44] which were all known to be related to the pathogenesis, progression, and resistance to therapy in CRC. Therefore, upon further validation, available inhibitors of these pathways with SOS1 inhibitor may provide the opportunities for rationale design of combination therapy trials for patients with CRC.

Our study on the cellular effect of BI3406 in CRC revealed potential cellular adaptation mechanisms. Rebound of GTP-bound RAS level at 48 hours upon treatment with BI3406 in not only resistant but also sensitive PDO models suggested that in resistant PDOs, inhibition of GEF function and downstream signaling could either be due to compensation from intrinsically activated alternative pathways such as those revealed above in the RNA-seq analysis, or from feedback upregulation of SOS1/2 expressions; In contrast, in sensitive PDOs, BI3406 induced antiproliferative effect at least may partially be due to off target activities such as those targets in the *MYC* and *E2F* pathways instead of *RTK/RAS* pathway. All these findings could be hypothesis generating and thus warrant dedicated studies. On the other hand, rationale combination therapy strategies should be extensively explored with known synergy between BI3406 and MEK inhibitor but should be expanded to agents targeting pathways other than *RTK/RAS*. In contrast to previous studies, our study utilized patient relevant PDO models to study the role of SOS1, specifically in CRC. We identified novel and rationale predictive biomarkers to the sensitivity of SOS1 inhibition and provided information on potential cellular adaptation mechanisms. These findings although may be important for future clinical development of SOS1-targeting agents, yet to overcome the limitations of our study, rigorous validations of these findings are required in patient-derived *in vivo* models or in correlative studies of clinical trials with large sample size that is statistically powered for biomarker discovery.

In summary, our study suggested that CRC PDOs could serve as better models for translational study of SOS1 in CRC. High SOS1 protein expression was a worse prognostic marker in CRC. High SOS1/SOS2 protein expression ratio predicted sensitivity to SOS1 inhibition and dependency. Our preclinical findings supported further clinical development of SOS1-targeting agents in CRC.

Supplementary Material

Refer to Web version on PubMed Central for supplementary material.

Acknowledgements

This study was supported by the Moffitt Cancer Center Support Grant to H. X., the Tissue Core, the Molecular Genomics Core, and the Biostatistics and Bioinformatics Shared Resource at the H. Lee Moffitt Cancer Center & Research Institute, an NCI designated Comprehensive Cancer Center (P30-CA076292). The Joan F. & Richard A. Abdoo Family Fund in Colorectal Cancer Research and CA265050 to M.E.F-Z.

Data availability statement

The data of this study are available from the corresponding author upon reasonable request.

References

1. Lakatos G, Köhne CH, Bodoky G. Current therapy of advanced colorectal cancer according to RAS/RAF mutational status. Cancer Metast Rev. Published online 2020:1–15. doi:10.1007/s10555-020-09913-7
2. Uprety D, Adjei AA. KRAS: From undruggable to a druggable Cancer Target. Cancer Treat Rev. 2020;89:102070. doi:10.1016/j.ctrv.2020.102070 [PubMed: 32711246]
3. Moore AR, Rosenberg SC, McCormick F, Malek S. RAS-targeted therapies: is the undruggable drugged? Nat Rev Drug Discov. 2020;19(8):533–552. doi:10.1038/s41573-020-0068-6 [PubMed: 32528145]
4. Freedman TS, Sondermann H, Friedland GD, et al. A Ras-induced conformational switch in the Ras activator Son of sevenless. Proc National Acad Sci. 2006;103(45):16692–16697. doi:10.1073/pnas.0608127103
5. Ooft SN, Weeber F, Dijkstra KK, et al. Patient-derived organoids can predict response to chemotherapy in metastatic colorectal cancer patients. Sci Transl Med. 2019;11(513):eaay2574. doi:10.1126/scitranslmed.aay2574 [PubMed: 31597751]
6. Pasch CA, Favreau PF, Yueh AE, et al. Patient-Derived Cancer Organoid Cultures to Predict Sensitivity to Chemotherapy and Radiation. Clin Cancer Res. 2019;25(17):5376–5387. doi:10.1158/1078-0432.ccr-18-3590 [PubMed: 31175091]
7. Vlachogiannis G, Hedayat S, Vatsiou A, et al. Patient-derived organoids model treatment response of metastatic gastrointestinal cancers. Science. 2018;359(6378):920–926. doi:10.1126/science.aao2774 [PubMed: 29472484]
8. clinicaltrials.gov. A Study to Test Different Doses of BI 1701963 Alone and Combined With Trametinib in Patients With Different Types of Advanced Cancer (Solid Tumours With KRAS Mutation). Accessed July 6, 2022. https://clinicaltrials.gov/ct2/show/NCT04111458
9. Hillig RC, Sautier B, Schroeder J, et al. Discovery of potent SOS1 inhibitors that block RAS activation via disruption of the RAS–SOS1 interaction. Proc National Acad Sci. 2019;116(7):2551–2560. doi:10.1073/pnas.1812963116
10. Hofmann MH, Gmachl M, Ramharter J, et al. BI-3406, a Potent and Selective SOS1–KRAS Interaction Inhibitor, Is Effective in KRAS-Driven Cancers through Combined MEK Inhibition. Cancer Discov. 2021;11(1):142–157. doi:10.1158/2159-8290.cd-20-0142 [PubMed: 32816843]
11. Sheffels E, Kortum RL. Breaking Oncogene Addiction: Getting RTK/RAS-Mutated Cancers off the SOS. J Med Chem. 2021;64(10):6566–6568. doi:10.1021/acs.jmedchem.1c00698 [PubMed: 33961431]
12. Lorenzi PL, Reinhold WC, Varma S, et al. DNA fingerprinting of the NCI-60 cell line panel. Mol Cancer Ther. 2009;8(4):713–724. doi:10.1158/1535-7163.mct-08-0921 [PubMed: 19372543]
13. Ianevski A, Giri AK, Aittokallio T. SynergyFinder 2.0: visual analytics of multi-drug combination synergies. Nucleic Acids Res. 2020;48(W1):W488–W493. doi:10.1093/nar/gkaa216 [PubMed: 32246720]
14. BLISS CI. THE TOXICITY OF POISONS APPLIED JOINTLY1. Ann Appl Biol. 1939;26(3):585–615. doi:10.1111/j.1744-7348.1939.tb06990.x

15. Yadav B, Wennerberg K, Aittokallio T, Tang J. Searching for Drug Synergy in Complex Dose–Response Landscapes Using an Interaction Potency Model. Comput Struct Biotechnology J. 2015;13:504–513. doi:10.1016/j.csbj.2015.09.001

16. Zhang DD, Hannink M. Distinct Cysteine Residues in Keap1 Are Required for Keap1-Dependent Ubiquitination of Nrf2 and for Stabilization of Nrf2 by Chemopreventive Agents and Oxidative Stress. Mol Cell Biol. 2003;23(22):8137–8151. doi:10.1128/mcb.23.22.8137-8151.2003 [PubMed: 14585973]

17. Kim MP, Evans DB, Wang H, Abbruzzese JL, Fleming JB, Gallick GE. Generation of orthotopic and heterotopic human pancreatic cancer xenografts in immunodeficient mice. Nat Protoc. 2009;4(11):1670–1680. doi:10.1038/nprot.2009.171 [PubMed: 19876027]

18. Roife D, Dai B, Kang Y, et al. Ex Vivo Testing of Patient-Derived Xenografts Mirrors the Clinical Outcome of Patients with Pancreatic Ductal Adenocarcinoma. Clin Cancer Res. 2016;22(24):6021–6030. doi:10.1158/1078-0432.ccr-15-2936 [PubMed: 27259561]

19. Evrard YA, Srivastava A, Randjelovic J, et al. Systematic Establishment of Robustness and Standards in Patient-Derived Xenograft Experiments and Analysis. Cancer Res. 2020;80(11):2286–2297. doi:10.1158/0008-5472.can-19-3101 [PubMed: 32152150]

20. van de Wetering M, Francies HE, Francis JM, et al. Prospective Derivation of a Living Organoid Biobank of Colorectal Cancer Patients. Cell. 2015;161(4):933–945. doi:10.1016/j.cell.2015.03.053 [PubMed: 25957691]

21. Miyoshi H, Stappenbeck TS. In vitro expansion and genetic modification of gastrointestinal stem cells in spheroid culture. Nat Protoc. 2013;8(12):2471–2482. doi:10.1038/nprot.2013.153 [PubMed: 24232249]

22. Klein M, Vignaud JM, Hennequin V, et al. Increased Expression of the Vascular Endothelial Growth Factor Is a Pejorative Prognosis Marker in Papillary Thyroid Carcinoma. J Clin Endocrinol Metabolism. 2001;86(2):656–658. doi:10.1210/jcem.86.2.7226

23. Bushnell B, Rood J, Singer E. BBMerge – Accurate paired shotgun read merging via overlap. Plos One. 2017;12(10):e0185056. doi:10.1371/journal.pone.0185056 [PubMed: 29073143]

24. Martin M Cutadapt removes adapter sequences from high-throughput sequencing reads. Embnet J. 2011;17(1):10–12. doi:10.14806/ej.17.1.200

25. Dobin A, Davis CA, Schlesinger F, et al. STAR: ultrafast universal RNA-seq aligner. Bioinformatics. 2013;29(1):15–21. doi:10.1093/bioinformatics/bts635 [PubMed: 23104886]

26. Li B, Dewey CN. RSEM: accurate transcript quantification from RNA-Seq data with or without a reference genome. Bmc Bioinformatics. 2011;12(1):323. doi:10.1186/1471-2105-12-323 [PubMed: 21816040]

27. Love MI, Huber W, Anders S. Moderated estimation of fold change and dispersion for RNA-seq data with DESeq2. Genome Biol. 2014;15(12):550. doi:10.1186/s13059-014-0550-8 [PubMed: 25516281]

28. Subramanian A, Tamayo P, Mootha VK, et al. Gene set enrichment analysis: A knowledge-based approach for interpreting genome-wide expression profiles. Proc National Acad Sci. 2005;102(43):15545–15550. doi:10.1073/pnas.0506580102

29. Cerami E, Gao J, Dogrusoz U, et al. The cBio Cancer Genomics Portal: An Open Platform for Exploring Multidimensional Cancer Genomics Data. Cancer Discov. 2012;2(5):401–404. doi:10.1158/2159-8290.cd-12-0095 [PubMed: 22588877]

30. Gao J, Aksoy BA, Dogrusoz U, et al. Integrative Analysis of Complex Cancer Genomics and Clinical Profiles Using the cBioPortal. Sci Signal. 2013;6(269):pl1. doi:10.1126/scisignal.2004088 [PubMed: 23550210]

31. Giannakis M, Mu XJ, Shukla SA, et al. Genomic Correlates of Immune-Cell Infiltrates in Colorectal Carcinoma. Cell Reports. 2016;15(4):857–865. doi:10.1016/j.celrep.2016.03.075 [PubMed: 27149842]

32. Hoadley KA, Yau C, Hinoue T, et al. Cell-of-Origin Patterns Dominate the Molecular Classification of 10,000 Tumors from 33 Types of Cancer. Cell. 2018;173(2):291–304.e6. doi:10.1016/j.cell.2018.03.022 [PubMed: 29625048]

33. Vasaikar S, Huang C, Wang X, et al. Proteogenomic Analysis of Human Colon Cancer Reveals New Therapeutic Opportunities. Cell. 2019;177(4):1035–1049.e19. doi:10.1016/j.cell.2019.03.030 [PubMed: 31031003]
34. Tsherniak A, Vazquez F, Montgomery PG, et al. Defining a Cancer Dependency Map. Cell. 2017;170(3):564–576.e16. doi:10.1016/j.cell.2017.06.010 [PubMed: 28753430]
35. Hogenson TL, Xie H, Phillips WJ, et al. Culture media composition influences patient-derived organoids ability to predict therapeutic response in gastrointestinal cancers. JCI Insight. 2022. doi:10.1172/jci.insight.158060.
36. Gurusamy N, Rajasingh S, Sigamani V, et al. Noonan syndrome patient-specific induced cardiomyocyte model carrying SOS1 gene variant c.1654A>G. Exp Cell Res. 2021;400(1):112508. doi:10.1016/j.yexcr.2021.112508 [PubMed: 33549576]
37. Roberts AE, Araki T, Swanson KD, et al. Germline gain-of-function mutations in SOS1 cause Noonan syndrome. Nat Genet. 2007;39(1):70–74. doi:10.1038/ng1926 [PubMed: 17143285]
38. Tartaglia M, Pennacchio LA, Zhao C, et al. Gain-of-function SOS1 mutations cause a distinctive form of Noonan syndrome. Nat Genet. 2007;39(1):75–79. doi:10.1038/ng1939 [PubMed: 17143282]
39. Sanchez-Vega F, Mina M, Armenia J, et al. Oncogenic Signaling Pathways in The Cancer Genome Atlas. Cell. 2018;173(2):321–337.e10. doi:10.1016/j.cell.2018.03.035 [PubMed: 29625050]
40. Sheffels E, Sealover NE, Wang C, et al. Oncogenic RAS isoforms show a hierarchical requirement for the guanine nucleotide exchange factor SOS2 to mediate cell transformation. Sci Signal. 2018;11(546):eaar8371. doi:10.1126/scisignal.aar8371 [PubMed: 30181243]
41. Nichols RJ, Haderk F, Stahlhut C, et al. RAS nucleotide cycling underlies the SHP2 phosphatase dependence of mutant BRAF-, NF1- and RAS-driven cancers. Nat Cell Biol. 2018;20(9):1064–1073. doi:10.1038/s41556-018-0169-1 [PubMed: 30104724]
42. Kuzu OF, Noory MA, Robertson GP. The Role of Cholesterol in Cancer. Cancer Res. 2016;76(8):2063–2070. doi:10.1158/0008-5472.can-15-2613 [PubMed: 27197250]
43. Solanki HS, Welsh EA, Fang B, et al. Cell Type–specific Adaptive Signaling Responses to KRASG12C Inhibition. Clin Cancer Res. Published online 2021. doi:10.1158/1078-0432.ccr-20-3872
44. Soleimani A, Rahmani F, Ferns GA, Ryzhikov M, Avan A, Hassanian SM. Role of the NF-κB signaling pathway in the pathogenesis of colorectal cancer. Gene. 2019;726:144132. doi:10.1016/j.gene.2019.144132 [PubMed: 31669643]

A.

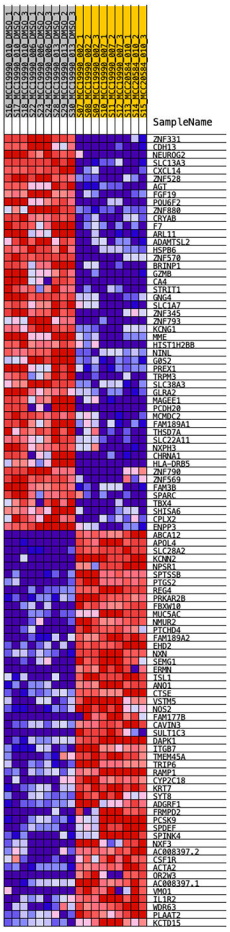

B.

CRC PDOs	KRAS status	IC_{50} (μM)
MCC19990-002	G12A	45.9
MCC19990-004	A146T	10.8
MCC19990-006	G12C	5.4
MCC19990-007	wild type	13.6
MCC19990-010	G12A	0.53
MCC19990-013	G12A	1.88
MCC20584-004	G12S	41.1
MCC20584-005	wild type	2.1
MCC20584-010	G12D	16.6

C.

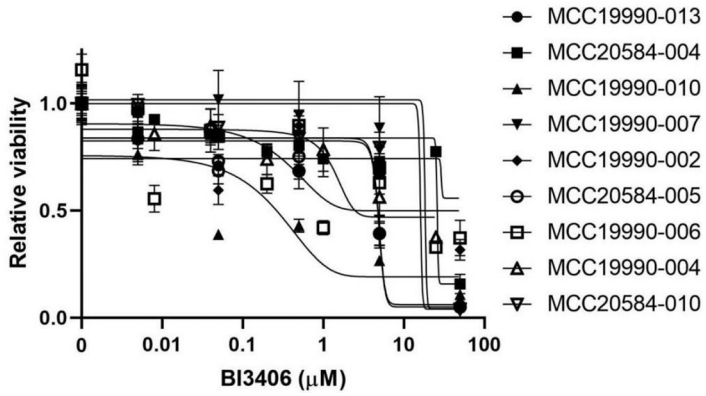

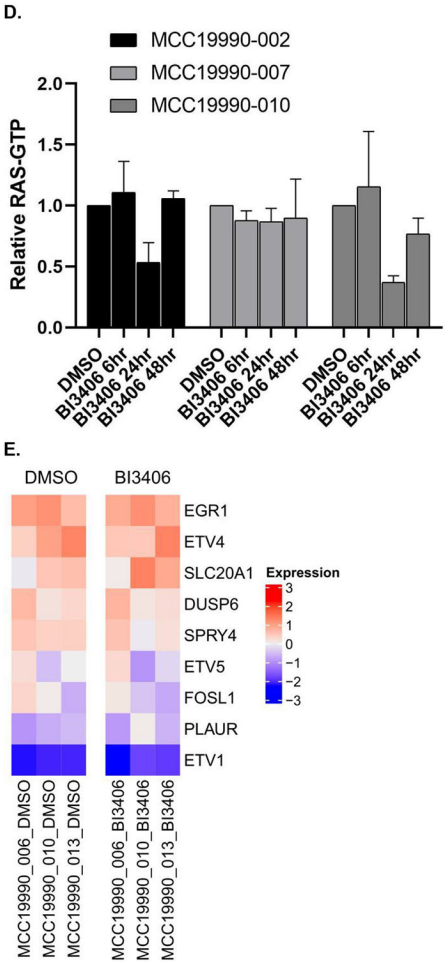

F.

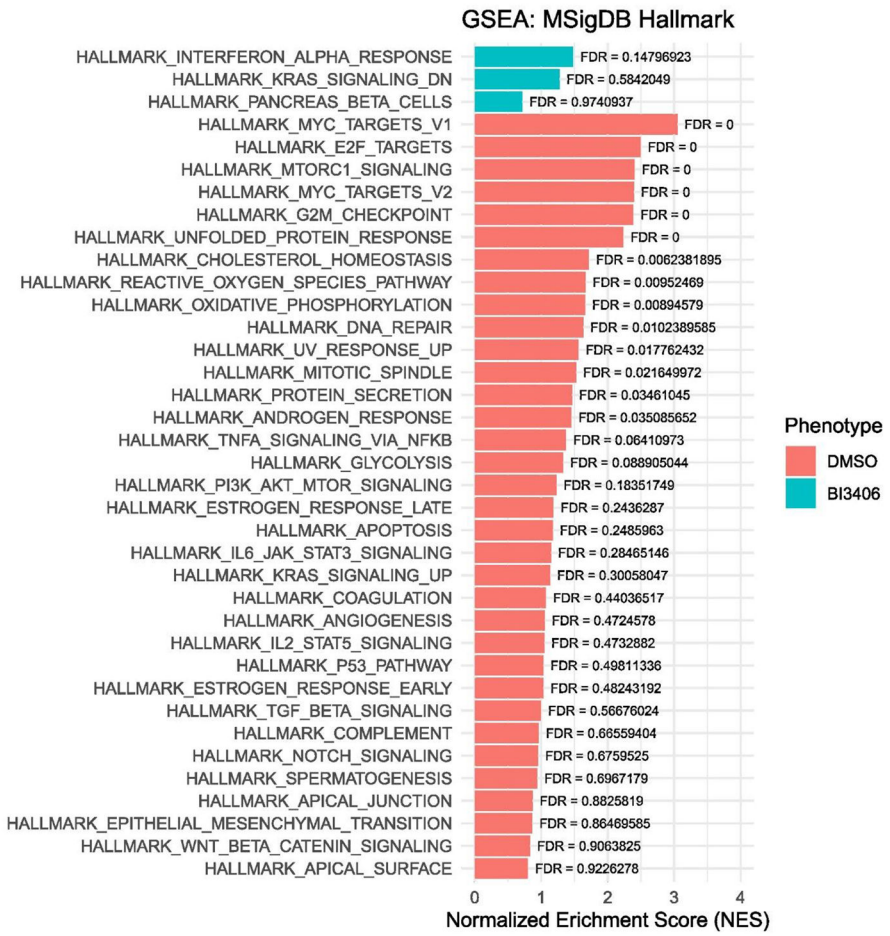

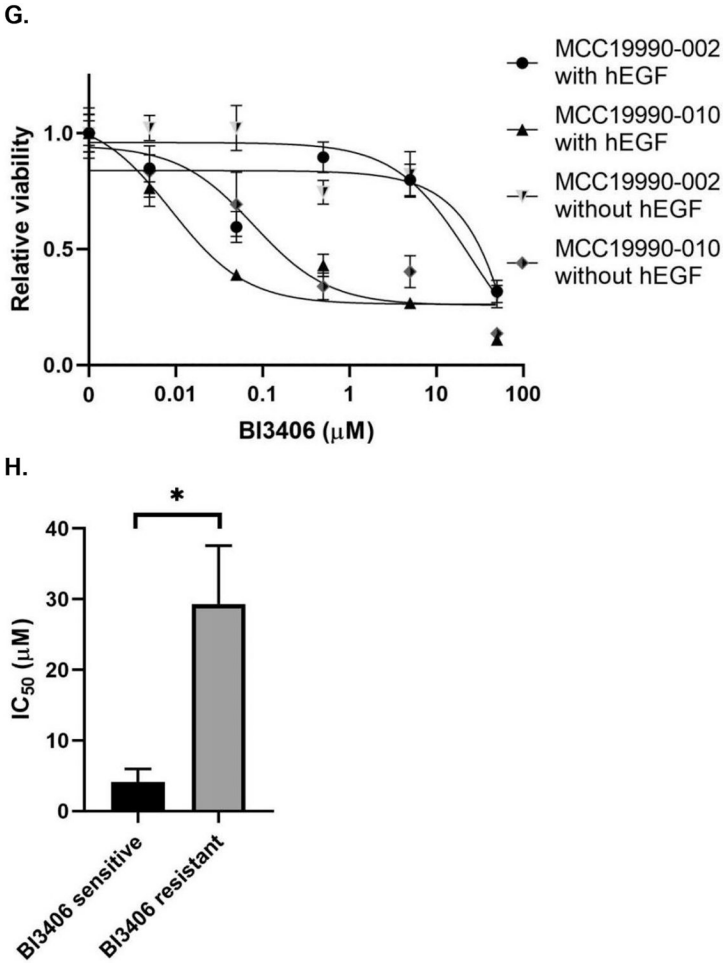

Figure 1.

Differential gene expression and effect of SOS1 inhibitor BI3406 in CRC PDOs. **(A)** Gene expressions of 6 CRC PDOs. The dataset has 19195 features (genes). Number of markers for phenotype sensitive: 9527 (49.6%) with correlation area 50.3%. Number of markers for phenotype resistant: 9668 (50.4%) with correlation area 49.7%. Heat Map included the top 50 features for each group of CRC PDOs. **(B)** IC_{50} values of BI3406 and *KRAS* mutation status in CRC PDOs. **(C)** Dose-response curves of CRC PDOs to BI3406. **(D)** GTP-bound KRAS levels in CRC PDOs after treatment with SOS1 inhibitor BI3406 at 0, 6, 24, and 48 hours. **(E)** Expression of 9 *KRAS* effector genes in BI3406 sensitive CRC PDOs before and after treatment with 1μM BI3406 for 24 hours. **(F)** Summary of GSEA of BI3406-sensitive CRC PDOs before and after treatment with 1μM BI3406 for 24 hours. **(G)** Dose-response curves of selected sensitive and resistant CRC PDOs to BI3406 in the presence or absence of human epidermal growth factor in the culture media. **(H)** Comparison of IC_{50} values of BI3406 in SOS1 inhibition sensitive and resistant CRC PDOs. p=0.016.

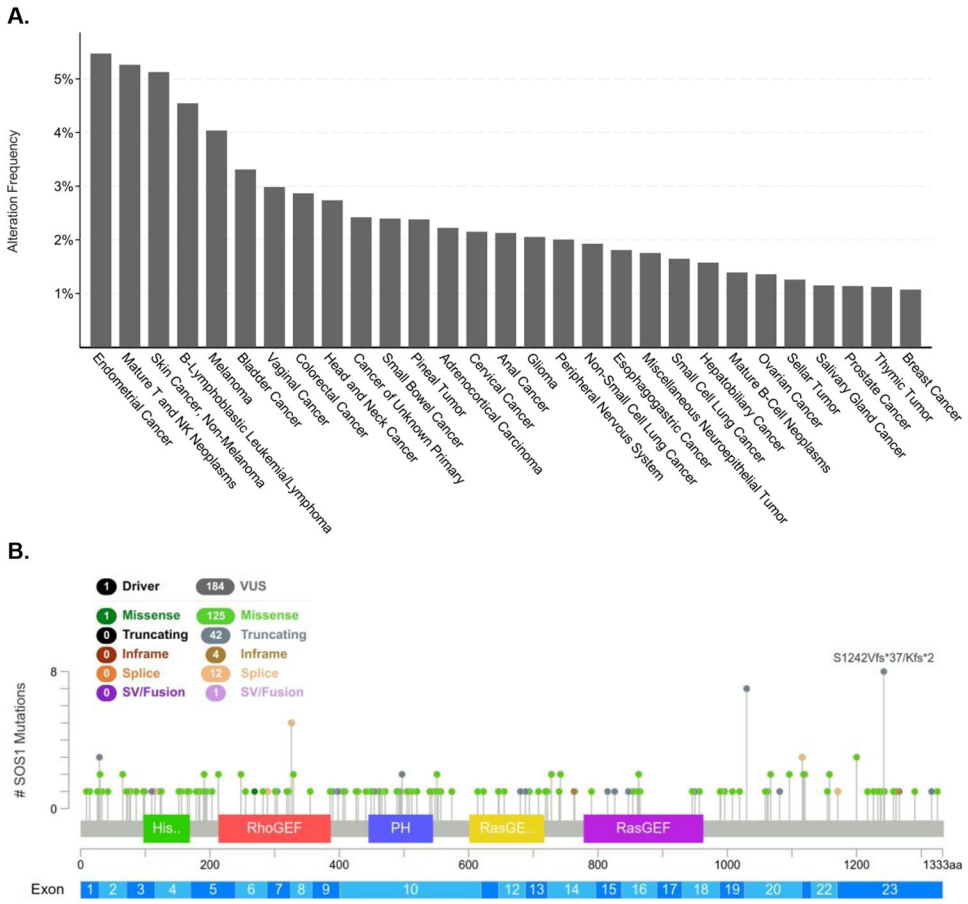

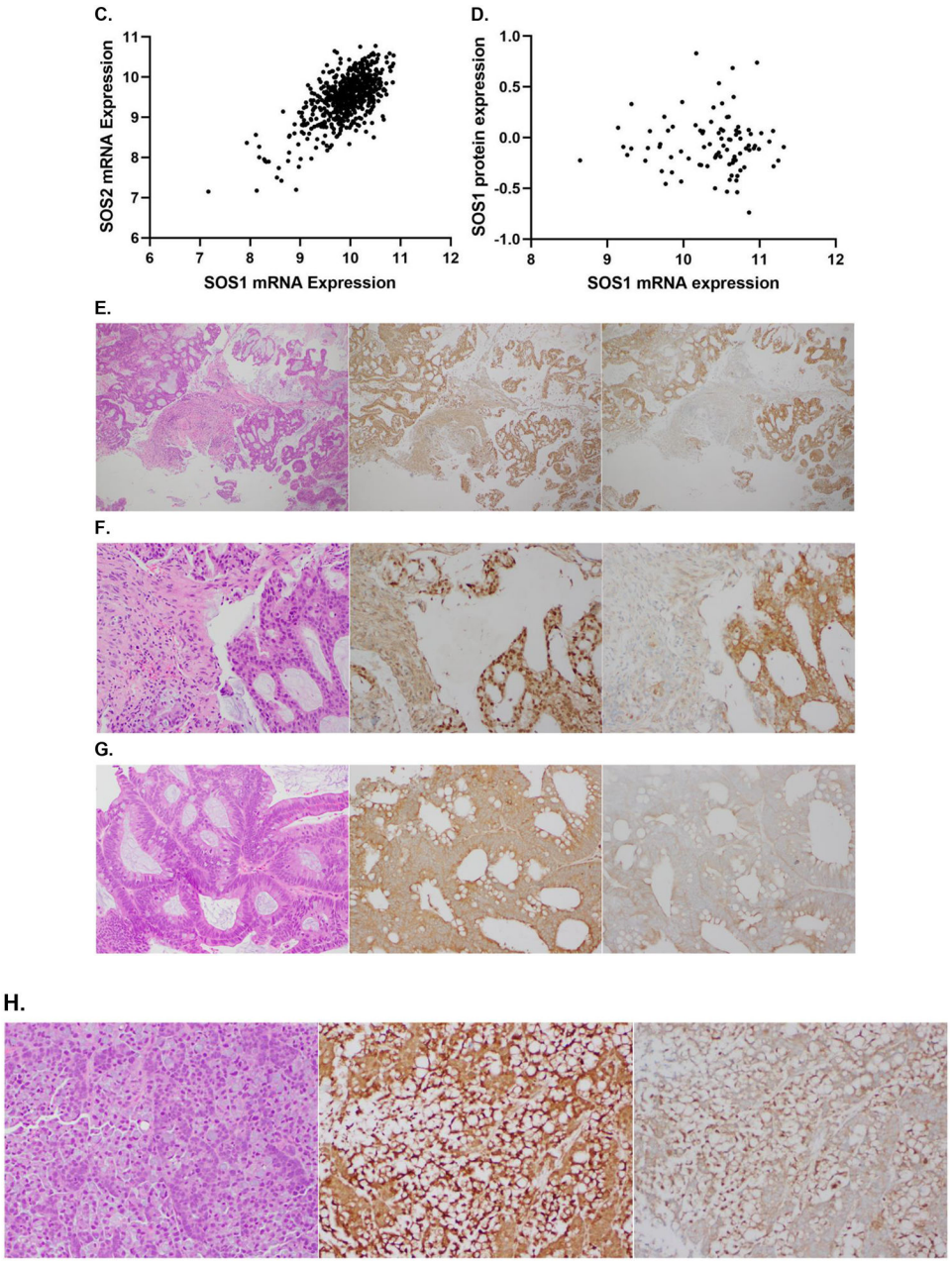

Figure 2.

Molecular alterations, mRNA, and protein expressions of SOS1 in CRC. **(A)** Prevalence of *SOS1* mutations across different cancer types in GENIE cohort v11.0. **(B)** Distribution of *SOS1* alterations in CRC. NM_005633 | ENST00000402219 CCDS1802 | SOS1_HUMAN in GENIE cohort v11.0. Putative drivers versus variants of unknown significance were determined by OncoKB and hotspots. **(C)** Correlation between *SOS1* and *SOS2* mRNA expressions (RSEM, Batch normalized from Illumina HiSeq_RNASeqV2, $\log_2$) in CRC in TCGA PanCancer Atlas. mRNA expression as $\log_2$(value + 1), Spearman's ρ: 0.56, p<0.001. **(D)** Correlation between *SOS1* mRNA (RSEM, Batch normalized from Illumina HiSeq_RNASeqV2, $\log_2$) and SOS1 protein expressions (mass spectrometry by CPTAC)

in CRC in CPTAC-2 Prospective (Cell 2019). Spearman's ρ: −0.05, p=0.6. **(E)** SOS1 and SOS2 expressions by IHC in CRC tissue in the low-power field. Left: H&E; Middle: SOS1 H-score 6; Right: SOS2 H-score 6. **(F)** SOS1 and SOS2 expressions by IHC in CRC tissue in the high-power field. Left: H&E; Middle: SOS1 H-score 6; Right: SOS2 H-score 6. **(G)** SOS1 and SOS2 expressions in moderately differentiated colon adenocarcinoma. Left: H&E; Middle: SOS1 H-score 6; Right: SOS2 H-score 3. **(H)** SOS1 and SOS2 expressions in poorly differentiated mucinous colon adenocarcinoma. Left: H&E; Middle: SOS1 H-score 9; Right: SOS2 H-score 6.

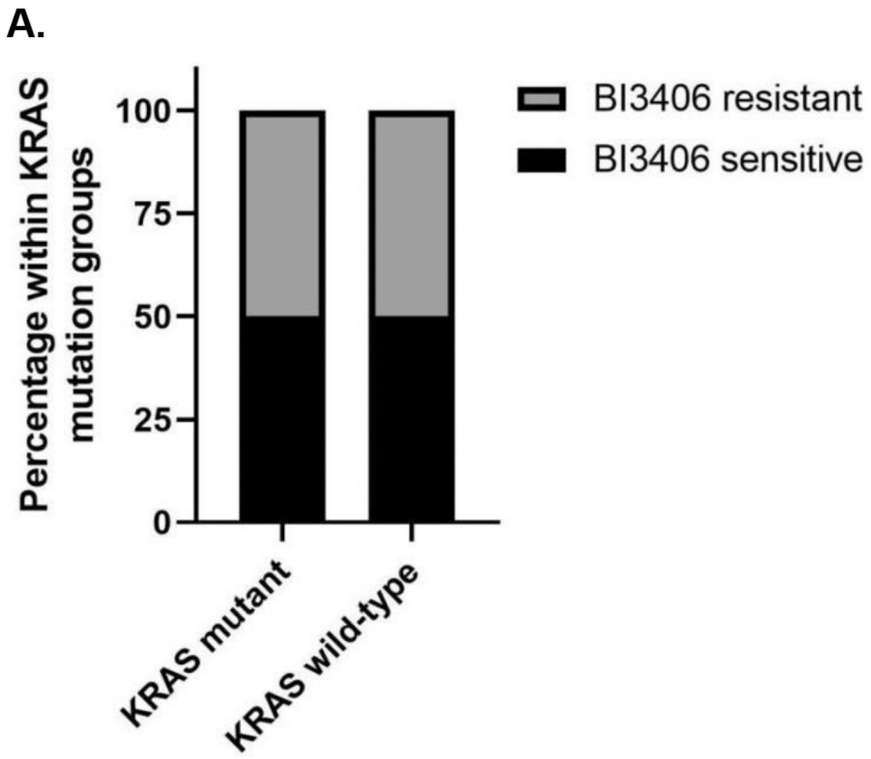

B.

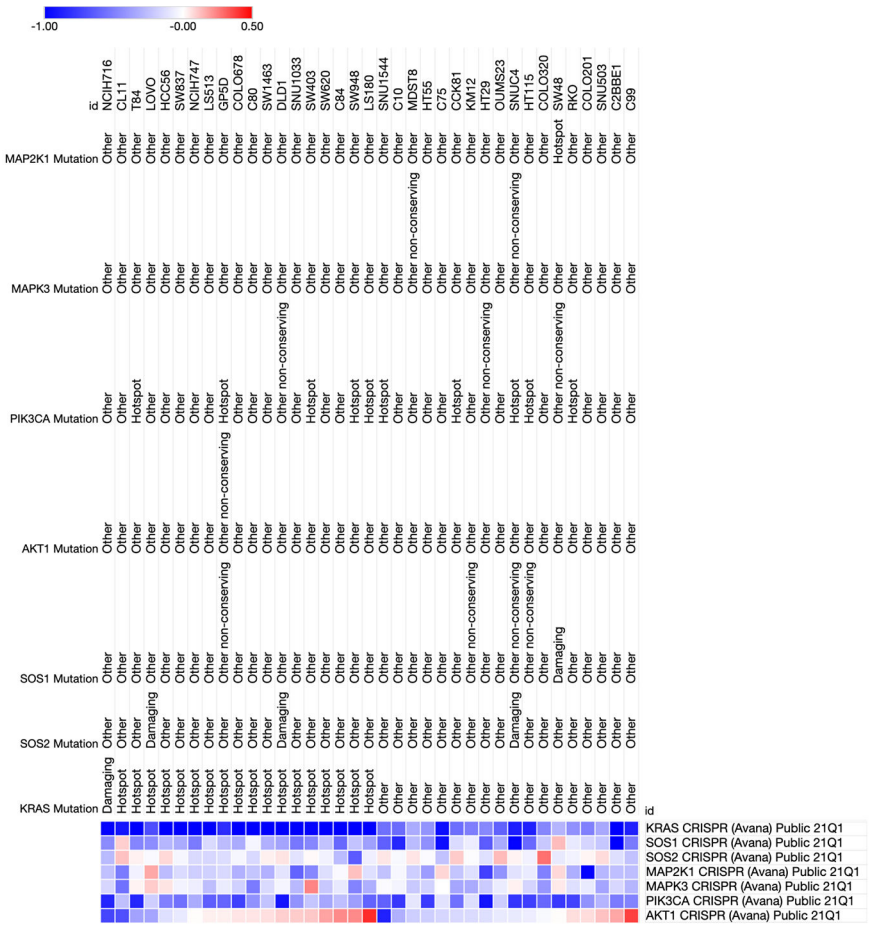

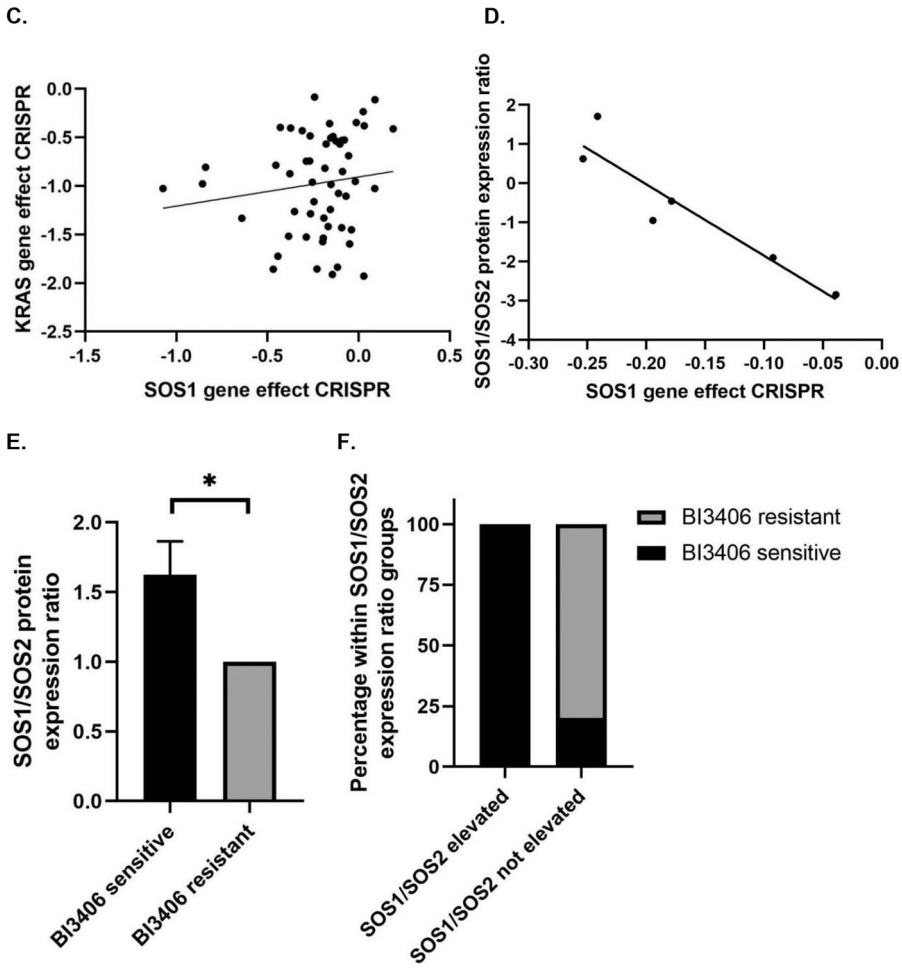

Figure 3.

Predictive markers to *SOS1* dependency and sensitivity to SOS1 inhibitor BI3406 in CRC models. **(A)** Association of BI3406 sensitivity with *KRAS* mutation status in CRC PDO. p=1. **(B)** Dependency of CRC cell lines to *SOS1* or *SOS2* knockout by CRISPR compared to other genes of *KRAS* signaling pathway in DepMap database. Dependency score less than zero suggests dependency of gene knockout. **(C)** Association of *SOS1* dependency with *KRAS* dependency in 54 CRC cell lines in DepMap database. Spearman's ρ: 0.18, p=0.2. **(D)** Association of SOS1/SOS2 protein expression ratio with *SOS1* dependency in DepMap database. Spearman's ρ: −0.886, p=0.007. **(E)** SOS1/SOS2 expression ratio by IHC in BI3406 sensitive and BI3406 resistant CRC PDXs. p=0.04. **(F)** The proportion of BI3406 sensitivity in SOS1/SOS2 expression ratio elevated and not elevated groups. The SOS1/SOS2 elevated group is defined as SOS1 H-score/SOS2 H-score >1. p=0.03.

A.

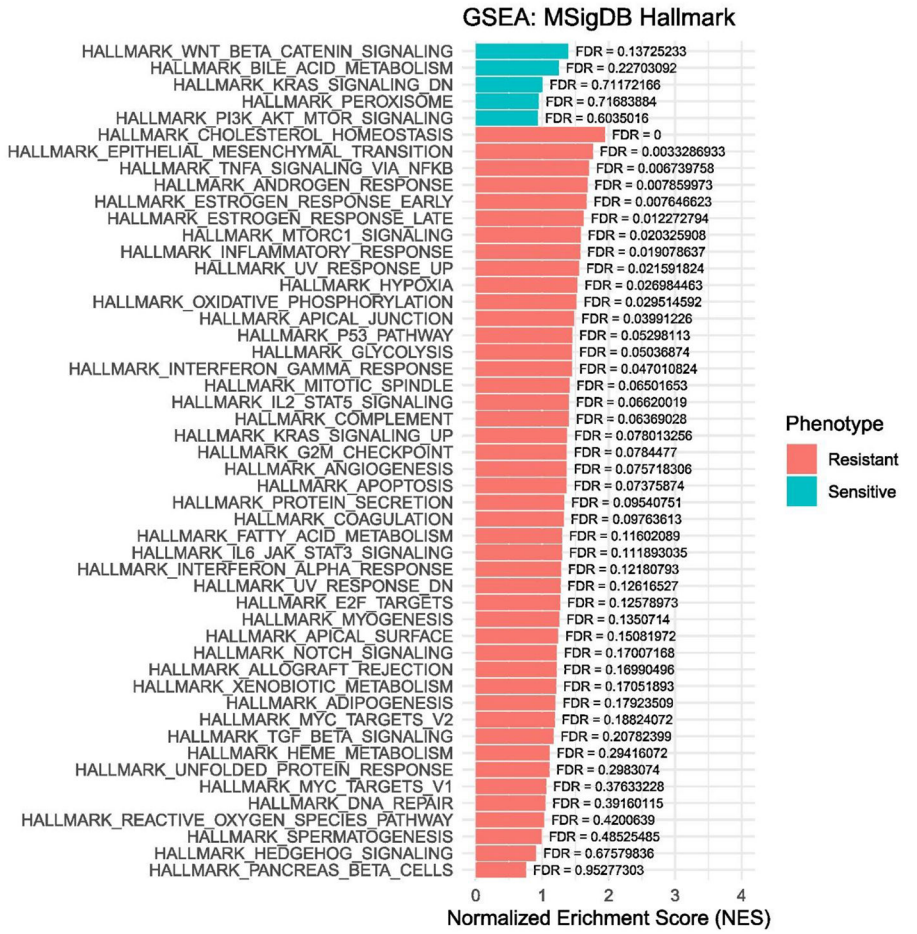

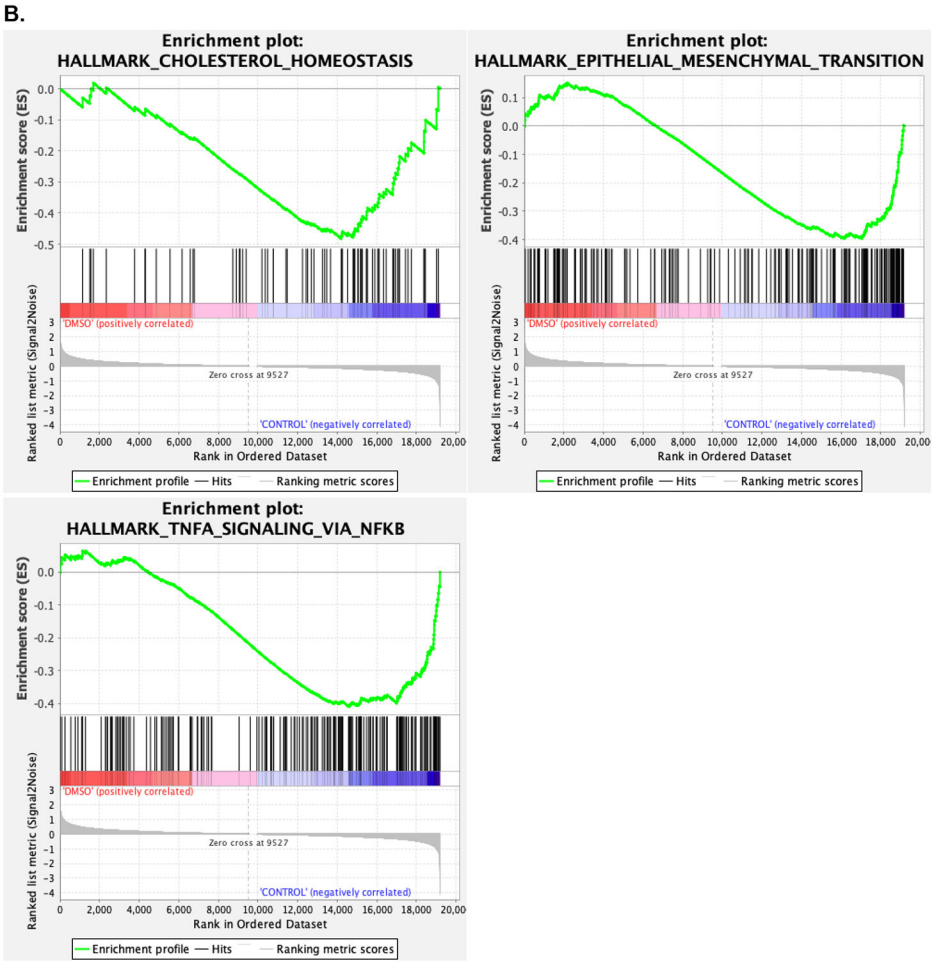

Figure 4.

Gene set enrichment analyses of mRNA expression in CRC PDOs. **(A)** Summary of GSEA of CRC PDOs with differential sensitivity to SOS1 inhibitor BI3406. **(B)** Enrichment plots in BI3406 sensitive vs resistant CRC PDOs. 39/50 gene sets are upregulated in phenotype resistant. 13 gene sets are significant enriched at FDR <25%. 7 gene sets are significantly enriched at nominal p value <1%. 11 gene sets are significantly enriched at nominal p value < 5%. 11/50 gene sets are upregulated in phenotype sensitive. 0 gene set is significantly enriched at FDR < 25%. 0 gene set is significantly enriched at nominal p value < 1%. 1 gene set is significantly enriched at nominal p value < 5%. Snapshots of enrichment results in resistant CRC PDOs are shown.